Materials Characterization 97 (2014) 161–168

Contents lists available at ScienceDirect

Materials Characterization

journal homepage: www.elsevier.com/locate/matchar

High-temperature tensile and creep deformation of cross-weld specimens of weld joint between T92 martensitic and Super304H austenitic steels

Myung-Yeon Kim [a,b], Suk-Chul Kwak [a], In-Suk Choi [a], Young-Kook Lee [b], Jin-Yoo Suh [a,*], Eric Fleury [a,c], Woo-Sang Jung [a], Tae-Ha Son [d]

[a] High Temperature Energy Materials Research Center, Korea Institute of Science and Technology, Seoul 136-791, Republic of Korea
[b] Department of Materials Science and Engineering, Yonsei University, Seoul 120-749, Republic of Korea
[c] Laboratoire d'Etude des Microstructures et de Mécanique des Matériaux, CNRS UMR 7239, Université de Lorraine, 57000 Metz, France
[d] Green Energy Laboratory, KEPCO Research Institute, Daejeon 305-760, Republic of Korea

ARTICLE INFO

Article history:
Received 16 September 2013
Received in revised form 4 September 2014
Accepted 21 September 2014
Available online 23 September 2014

Keywords:
Heat-resistant steel
Welding
Heat-affected zone
Hardness measurement
Laves phase
Electron microscopy

ABSTRACT

The high-temperature mechanical behavior of cross-weld specimens prepared from a dissimilar weld joint between T92 martensitic and Super304H austenitic heat-resistant steels incorporating Ni-based weld metal was evaluated at temperatures up to 650 °C. For both high temperature tensile and creep tests, failure took place in T92 due to its faster degradation with temperature increase. The heat-affected zone of T92 played a critical role during creep deformation, resulting in type IV failure under the long-term creep condition. For the creep specimens, the location of failure shifted from the base metal region to the fine-grained heat-affected zone as the creep duration time increased from the short-term to the long-term condition. The massive precipitation of Laves phase on the grain boundaries of the fine-grained heat-affected zone during creep deformation was observed and found to be responsible for the accelerated void formation in the area leading to the premature failure.

1. Introduction

The welding of different metallic materials is an important procedure for building engineering structures exhibiting both high functionality and cost efficiency. Boiler units of the advanced coal-fired power plants also have a lot of weld joints between different metals, for example, weld joints between a stable austenitic heat-resistant steel and a cost-effective but less stable martensitic heat-resistant steel. However, the welding process is bound to create a heat-affected zone (HAZ) in base metals (BM) as well as a rapidly solidified microstructure in weld metals (WM). Because a variation in microstructure significantly affects the mechanical response of a material, careful investigation of the microstructure–property relationship of weld joints should be conducted prior to any actual application.

The HAZ of martensitic heat-resistant steels is reported to degrade under long-term creep, resulting in a brittle failure called type IV fracture in grade 91 [1,2], grade 92 [3,4], and grade 122 [1,3–6] steels. The type IV failure was also reported from the cross-weld specimens extracted from dissimilar weld joints of T92/HR3C [7,8] and T91/TP316H [9]. For the dissimilar weld joints, premature failure always occurs in martensitic steels, not in austenitic steels, indicating the accelerated degradation of the HAZ in martensitic steels. The type IV failure is generally attributed to grain refinement, which is caused by a martensite → austenite → martensite phase transition occurring during the welding thermal cycle, resulting in a fine-grained zone in the HAZ (FGHAZ) [10]. In this region, partial dissolution of grain boundary carbides such as $M_{23}C_6$ (M stands for 'metal' and major metallic element constituting $M_{23}C_6$ is Cr) also takes place during the welding. The dissolved Cr and C precipitate back preferentially on the remaining particles during creep service to result in large precipitates [10,11]. The accelerated precipitation and growth of the grain boundary carbides have two effects: (i) the softening of the matrix by the depletion of solid-solution strengtheners and (ii) the preferred nucleation of creep voids at the matrix–precipitate interface due to the inconsistent plastic strain between the matrix and coarsened precipitates. Additionally, faster softening of a limited area could create stress triaxiality due to the geometrical confinement of the softened region, which is sandwiched between harder regions [1,12]. Stress triaxiality is known to accelerate void formation in this specific area.

Despite many studies on the type IV failure, the detailed mechanism explaining why the creep properties of the HAZ are inferior to those of the base metal has not yet been elucidated. For example, it is still unclear regarding which type of grain boundary precipitate is responsible

* Corresponding author.
E-mail address: jinyoo@kist.re.kr (J.-Y. Suh).

http://dx.doi.org/10.1016/j.matchar.2014.09.011
1044-5803/

for the type IV failure: $Cr_{23}C_6$ [3] and Z-phase [4] were discussed as critical factors affecting the degradation. In addition, recent reports on similar material systems, T92/HR3C [7] and T91/TP316H [9], are in disagreement with each other regarding the location of type IV failure. In this context, the present study aimed to provide a detailed description of the microstructure–property relationship of dissimilar weld joints between T92 and Super304H (S304H). In addition to the creep-rupture experiments, high-temperature tensile properties were evaluated to understand the basic mechanical behavior of the dissimilar weld joint. Hardness measurements were performed along a line crossing the HAZ in T92 martensitic steel specimens before and after creep tests. Finally, a transmission electron microscope (TEM) and an electron probe micro-analyzer (EPMA) were used to characterize the microstructural degradation of the HAZ. For some TEM specimens, special care was applied to extract from the area as close to the fracture surface as possible using focused ion beam (FIB) milling.

2. Experimental

Table 1 shows the chemical compositions of the steels used in the present study. The concentration of minor impurities such as P and S was also included since they are known to affect the intergranular cracking [13,14]. For WM, a Ni-based alloy, ERNiCr-3 ($18 < Cr < 22$, $C < 0.1$, $2.5 < Mn < 3.5$, $2 < Nb < 3$, $Fe < 3$, $Cu < 0.5$, $Si < 0.5$, $P < 0.03$, $S < 0.015$ in wt.%), was used. Tubes with dissimilar weld joints produced via multi-pass gas tungsten arc welding (GTAW, 5 pass) were provided by Doosan Heavy Industry Company, Korea. The welding current, voltage, and speed ranged from 80 to 130 A, 10 to 13 V, and 6 to 8 cm/min, respectively. The welded tubes were post-weld heat-treated (PWHT) at 750 °C for 90 min. Fig. 1(a) shows a drawing and a photograph of the welded tubes. Cross-weld specimens for high-temperature tensile testing were machined to the dimensions of 4 mm in diameter and 25 mm in gage length (ASTM E8). Creep specimens were machined to 6.35 mm in diameter and 32 mm in gage length (ASTM E139). Fig. 1(b) shows a creep specimen that was slightly etched to reveal the boundaries of S304H/WM and WM/T92. To observe the microstructure of the T92 component, a mixture of hydrochloric acid (5 ml) and picric acid (4 g) in methanol (100 ml) was used (based on method 80 detailed in ASTM E 407-07). FEI Tecnai F20, FEI Inspect F50, and JEOL JXA-8500F were used for TEM, SEM, and EPMA analyses, respectively.

3. Results and discussions

3.1. High-temperature tensile behavior

Fig. 2 shows the engineering stress–strain curves acquired by tensile tests on T92, S304H, and cross-weld specimens performed at room temperature (RT), 550, 600, and 650 °C at a strain rate of 10^{-4} s^{-1} (corresponding to the crosshead speed of 0.0025 mm/s). The tensile behavior of the individual base metals revealed an obvious contrast between the T92 and S304H metals. S304H showed typical yielding and strain-hardening behavior both at room and high temperatures; the metal exhibited a relatively low yield stress and the high degree of strain hardening to reach a high level of ultimate tensile stress. On the other hand, T92 is a martensitic steel characterized by laths with a high dislocation density and, thus, exhibits a high yield stress but softening during plastic deformation [15]. Therefore, plastic deformation of the cross-weld specimens was initiated by the yielding of S304H for RT, 550, and 600 °C. On the

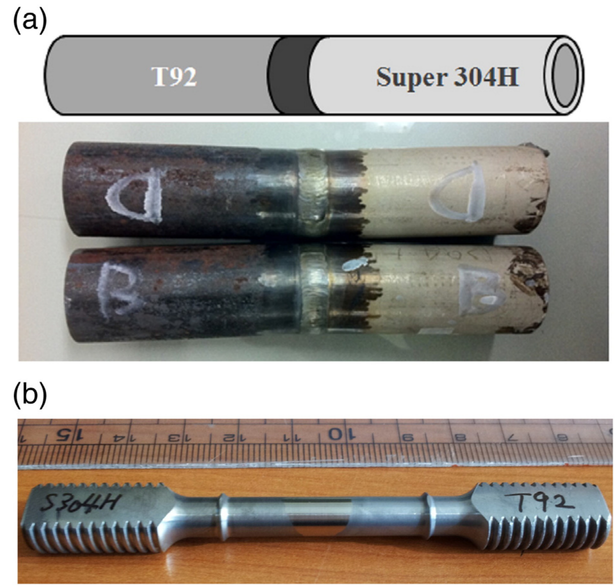

Fig. 1. (a) Welded tubes between T92 and S304H with ERNiCr-3 as WM. (b) A creep specimen that was slightly etched to show the boundaries of S304H/WM and WM/T92.

other hand, the final stage of the tensile deformation was dominated by that of T92. It is obvious that the T92 softens faster than S304H with temperature increase to have the similar yield stress to that of S304H at 650 °C. The location of failure was in the base metal region of T92 for all temperatures except room temperature. At room temperature, failure occurred inside the Ni-based WM. All tests on the cross-weld specimens were carried out twice and showed reasonable reproducibility.

3.2. Creep behavior

Fig. 3 and Table 2 show creep-rupture data obtained at temperatures of 600 and 650 °C. The creep data sheet issued by the National Institute of Materials Science (NIMS, Japan) was used as a reference for the creep properties of individual base metals T92 and S304H [16]. Tests on the base metals were also carried out to ensure consistency between the data collected in this study and those in the NIMS data sheet. The creep-rupture data of the cross-weld specimens turned out to replicate those of T92 for the short-term creep condition. However, as the duration time increased by lowering the initial load, the cross-weld specimens started to show a clear deviation; the rupture data denoted '600-4' (600 °C, 150 MPa) and '650-5' (650 °C, 75 MPa) in Fig. 3(a) and (b), respectively, deviated from the expected behavior owing to the premature failure. The degradation that has occurred under the long-term creep condition appears even more obvious when the images of the specimens fractured under different conditions and their fracture surfaces are compared as shown in Fig. 4. In Fig. 4(a), for the specimens submitted to tensile testing and short-term creep testing with a higher initial load (denoted as 600-1 and 600-3 in Figs. 3(a) and 4), ductile fracture with a significant amount of necking was observed. However, the specimen ruptured by a stress of 150 MPa at 600 °C (denoted as 600-4 in Figs. 3(a) and 4) showed clear brittle fracture accompanying no reduction of area. The fracture surface of the '600-4' specimen appears parallel to the fusion line of welding, the boundary between T92 and WM, which suggests

Table 1
Chemical compositions of T92 and S304H in wt.%.

	C	Cr	Ni	Mn	Si	Mo	V	Nb	W	Cu	Al	S	P	N	B
T92	0.13	9.04	0.18	0.54	0.26	0.42	0.19	0.04	0.8	0.11	0.01	0.003	0.024	0.07	0.003
S304H	0.098	18.69	8.66	0.79	0.29	0.29	0.05	0.47		3.1	0.01	<0.001	0.041	0.12	0.005